

Structural and Physical Properties of the 6M BaIrO<sub>3</sub>: A New Metallic Iridate Synthesized under High PressureJinggeng Zhao,<sup>\*,†,‡</sup> Liuxiang Yang,<sup>†</sup> Yong Yu,<sup>†</sup> Fengying Li,<sup>†</sup> Richeng Yu,<sup>†</sup> and Changqing Jin<sup>†</sup>

Beijing National Laboratory for Condensed Matter Physics, Institute of Physics, Chinese Academy of Sciences, Beijing 100190, P. R. China, and Natural Science Research Center, Academy of Fundamental and Interdisciplinary Sciences, Harbin Institute of Technology, Harbin 150080, P. R. China

Received September 5, 2008

The 6M BaIrO<sub>3</sub> with the distorted hexagonal BaTiO<sub>3</sub> structure was synthesized by high-pressure sintering. Through Rietveld refinement of the powder X-ray diffraction data, the lattice parameters of  $a = 5.7459(1) \text{ \AA}$ ,  $b = 9.9289(2) \text{ \AA}$ ,  $c = 14.3433(2) \text{ \AA}$ , and  $\beta = 91.340(1)^\circ$  were obtained. In the Ir<sub>2</sub>O<sub>9</sub> dioctahedron, the average Ir–O distance and direct Ir–Ir distance were equal to 2.067(19) and 2.719(1) Å, respectively. The temperature dependence of electrical resistivity shows that the 6M BaIrO<sub>3</sub> is a new metallic iridate. It is an abnormal metal, being deviated from the Fermi liquid behavior, following a linear relationship of  $\rho$  versus  $T$  below 20 K. Both magnetic susceptibility and specific heat data indicate that it is an exchange-enhanced Pauli paramagnet, because of the electron–electron correlation effect.

## Introduction

The oxide ruthenates have received growing attention for their exotic physical properties. For example, Sr<sub>2</sub>RuO<sub>4</sub> is a superconductor of unconventional p-wave pairing mechanism.<sup>1</sup> The oxide iridates are very similar with ruthenates in unique structural and physical properties. The ambient pressure phase of BaIrO<sub>3</sub> is the first known ferromagnet that contains a 5d transition metal cation in a ternary oxide, with the Curie temperature  $T_c$  about 183 K.<sup>2</sup> Sr<sub>2</sub>IrO<sub>4</sub> and Sr<sub>3</sub>Ir<sub>2</sub>O<sub>7</sub>, which adopt the distorted Ruddlesden–Popper structure,<sup>3,4</sup> are also weak ferromagnets, with  $T_c$  values of about 250 and 290 K, respectively.<sup>5,6</sup>

In the alkaline-earth oxide iridate AIrO<sub>3</sub> (A = Ca, Sr, and Ba), the structural and physical property strongly depend on the size of A site cations and synthesis conditions. CaIrO<sub>3</sub> crystallizes into the postperovskite structure with the space group *Cmcm*.<sup>7</sup> It is an antiferromagnetic insulator.<sup>8</sup> SrIrO<sub>3</sub> adopts the distorted hexagonal BaTiO<sub>3</sub>-type structure with the space group *C2/c* at ambient condition,<sup>9</sup> which is denoted as 6M for its similar structure with the 6H BaTiO<sub>3</sub>. It is a paramagnetic metal. Under high temperature and high pressure, SrIrO<sub>3</sub> transforms to an orthorhombic perovskite-type oxide with the space group *Pnma*.<sup>9</sup> BaIrO<sub>3</sub> crystallizes into the monoclinic structure at ambient condition, with the space group *C2/m*, rather than the rhombohedral structure,<sup>10</sup> because of a large tolerant factor (about 1.051) as calculated from the ionic radii in the Shannon table.<sup>11</sup> The ion coordination of BaIrO<sub>3</sub> is similar to that of the 9R BaRuO<sub>3</sub>, so it is denoted as 9M. It is the first known ferromagnet with a Curie temperature  $T_c$  value of about 183 K,<sup>2</sup> which originates from spin polarization of Ir cations rather than

\* To whom correspondence should be addressed. Tel.: 86-10-82648041; Fax.: 86-10-82640223. E-mail: zhaojinggeng@163.com.

<sup>†</sup> Institute of Physics, Chinese Academy of Sciences.

<sup>‡</sup> Harbin Institute of Technology.

- (1) Maeno, Y.; Hashimoto, H.; Yoshida, K.; Nishizaki, S.; Fujita, T.; Bednorz, J. G.; Lichtenberg, F. *Nature (London)* **1994**, *372*, 532–534.
- (2) Lindsay, R.; Strange, W.; Chamberland, B. L.; Moyer, R. O., Jr. *Solid State Commun.* **1992**, *86*, 759–763.
- (3) Huang, Q.; Soubeyroux, J. L.; Chmaissem, O.; Sora, L. N.; Santoro, A.; Cava, R. J.; Krajewski, J. J.; Peck, W. F., Jr. *J. Solid State Chem.* **1994**, *112*, 355–361.
- (4) Matsuhata, H.; Nagai, I.; Yoshida, Y.; Hara, S.; Ikeda, S.-I.; Shirakawa, N. *J. Solid State Chem.* **2004**, *177*, 3776–3783.
- (5) Crawford, M. K.; Subramanian, M. A.; Harlow, R. L.; Fernandez-Baca, J. A. *Phys. Rev. B* **1994**, *49*, 9198–9201.
- (6) Nagai, I.; Ikeda, S.-I.; Yoshida, Y.; Kito, H.; Shirakawa, N. *J. Low Temp. Phys.* **2003**, *131*, 665–669.

(7) Rodi, F.; Babel, D. Z. *Anorg. Allg. Chem.* **1965**, *336*, 17–23.

(8) Ohgushi, K.; Gotou, H.; Yagi, T.; Kiuchi, Y.; Sakai, F.; Ueda, Y. *Phys. Rev. B* **2006**, *74*, 241104.

(9) Longo, J. M.; Kafalas, J. A.; Arnott, R. J. *J. Solid State Chem.* **1971**, *3*, 174–179.

(10) Siegrist, T.; Chamberland, B. L. *J. Less-Common Met.* **1991**, *170*, 93–99.

(11) Shannon, R. D. *Acta Crystallogr., Sect. A* **1976**, *32*, 751–767.

spin canting.<sup>12–14</sup> The notations of 9R, 4H, and 6H are related to BaRuO<sub>3</sub>,<sup>15</sup> in which Ba and O ions can form BaO<sub>3</sub> layer by close stacking mode. The Ru cation fills the interspace of O anions, which form RuO<sub>6</sub> octahedrons. The two modes of stacking between the two adjacent BaO<sub>3</sub> layers are hexagonal close stacking and cubic close stacking, which corresponds to the face-shared and corner-shared connections between the two neighboring RuO<sub>6</sub> octahedrons, respectively. The 9R, 4H, and 6H are the three types of hexagonal perovskite-type BaRuO<sub>3</sub>, where the number is the amount of BaO<sub>3</sub> layers in a unit cell, and the R and H denote the rhombohedral and hexagonal structures, respectively.

Komer et al. claimed that they had obtained the 4H BaIrO<sub>3</sub> by using high-pressure synthesis method.<sup>16</sup> However, they did not report the data of crystal structure and physical properties of the 4H BaIrO<sub>3</sub> for the mixture with the 9M form in their sample. In fact, the undistorted or distorted 6H BaTiO<sub>3</sub> forms of BaIrO<sub>3</sub> could be easily obtained at ambient pressure with chemical substitution of 1/3 M cations (M = alkali metals, alkaline earth elements, 3d transition metals, and lanthanides) for Ir ion, denoted as Ba<sub>3</sub>MIr<sub>2</sub>O<sub>9</sub>, in which the Ir and M ions occupy the Ir<sub>2</sub>O<sub>9</sub> dioctahedron and MO<sub>6</sub> octahedron, respectively.<sup>17–19</sup> All the doping compounds are semiconductors.<sup>17–20</sup> However, the physical or structural properties of the 6M BaIrO<sub>3</sub> have not been available so far, and there is no any report about the single-phase 6M BaIrO<sub>3</sub> up to now. For the first time, we report the structural detail based on Rietveld refinement and the systematic characterization of unconventional electrical and magnetic properties of the 6M BaIrO<sub>3</sub>.

## Experimental Section

**Synthesis.** The 9M BaIrO<sub>3</sub> was synthesized by using the conventional solid-state chemical reaction.<sup>21</sup> The starting materials were barium carbonate and iridium metal of 99.9% purity. Stoichiometric quantities of materials were mixed together, ground about 30 min in an agate mortar, and placed into an Al<sub>2</sub>O<sub>3</sub> crucible. The powder was then calcined for about 12 h at 900 °C in air. The calcined powder was reground, pressed into a pellet at the pressure of 10 MPa, and sintered at 1000 °C for about 72 h in air with two intermediate grindings. The XRD data in ref 21 indicate that the 9M BaIrO<sub>3</sub> sample is pure for the further research. The 6M SrIrO<sub>3</sub> was also synthesized using a similar method.<sup>22</sup>

The 6M BaIrO<sub>3</sub> was obtained using a conventional cubic-anvil type high-pressure facility. The 9M form was pressed into a pellet

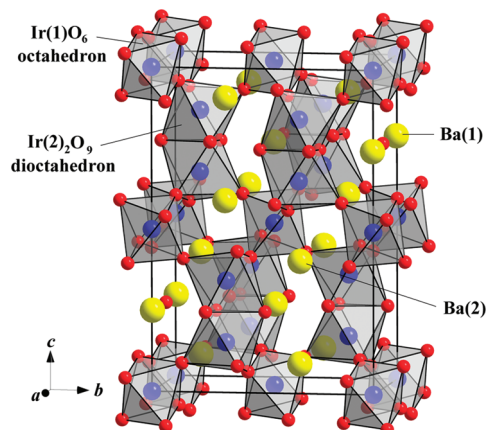


**Figure 1.** Schematic view of the 6M BaIrO<sub>3</sub>. The IrO<sub>6</sub> octahedrons are represented by geometrical figures (Ir at the center, O at corners). The unit cells are outlined.

of 5.0 mm diameter and then wrapped with gold foil to avoid contamination. The pellet was put into an h-BN sleeve, which was in turn inserted into a graphite tube heater. Pyrophyllite was used as the pressure-transmitting medium. The treating process was carried out at 5.0 GPa and 1000 °C for about 30 min, followed by a quench from high temperature before releasing pressure with the rate about 0.6 GPa/min.

We also obtained an uncertain structure of BaIrO<sub>3</sub>, which may be intervenient the 9M and 6M forms, at 3.3–4.0 GPa and 1000 °C. When the synthesis pressure is smaller than 3.3 GPa, BaIrO<sub>3</sub> maintains its primal structure of the 9M form. There is no a similar structure of BaIrO<sub>3</sub> with the 4H BaRuO<sub>3</sub>.

**X-ray Diffraction Analysis.** The structure of our sample was checked by the powder X-ray diffraction (XRD) with Cu-K<sub>α</sub> radiation at room temperature, using a Rigaku diffractometer (MXP-AHP18). The experimental data were collected in 2θ steps of 0.02° and 3 s counting time in the range 10° ≤ 2θ ≤ 120° and analyzed with the Rietveld method by using the FullProf program.<sup>23</sup>

**Electrical Resistivity Measurements.** The measurement of temperature dependences of electrical resistivity were performed by using the four-probe method with Ag paste contacts on an Oxford Maglab measuring system in the temperature range 3–300 K.

**Magnetic Susceptibility Measurements.** The relationships of magnetic susceptibility versus temperature were obtained using a SQUID magnetometer (Quantum Design, MPMS-5S) in the range 5–300 K. Data were collected under both zero-field-cooled (ZFC) and field-cooled (FC) conditions in the applied field of 1 T. The magnetic field dependence of magnetization was measured at 5 K in the range 0–5 T.

**Specific Heat Measurements.** The heat-capacity measurement was carried out using a heat pulse relaxation technique by a commercial heat capacity measuring system (Quantum Design, PPMS equipment) in the range 2–30 K. The sample was mounted on a thin alumina plate with grease for better thermal contact.

## Results and Discussion

**Crystal Structure.** The schematic view of the crystallographic form of the 6M BaIrO<sub>3</sub> is shown in Figure 1. In the 6M structure, two adjacent IrO<sub>6</sub> octahedrons stack together with face-shared connections to form one Ir<sub>2</sub>O<sub>9</sub> dioctahedron, and the IrO<sub>6</sub> octahedron and Ir<sub>2</sub>O<sub>9</sub> dioctahedron

- (12) Cao, G.; Crow, J. E.; Guertin, R. P.; Henning, P. F.; Homes, C. C.; Strongin, M.; Basov, D. N.; Lochner, E. *Solid State Commun.* **2000**, *113*, 657–662.
- (13) Brooks, M. L.; Blundell, S. J.; Lancaster, T.; Hayes, W.; Pratt, F. L.; Frampton, P. P. C.; Battle, P. D. *Phys. Rev. B* **2005**, *71*, 220411.
- (14) Nakano, T.; Terasaki, I. *Phys. Rev. B* **2006**, *73*, 195106.
- (15) Longo, J. M.; Kafalas, J. A. *Mater. Res. Bull.* **1968**, *3*, 687–692.
- (16) Komer, W. D.; Machin, D. J. *J. Less-Common Met.* **1978**, *61*, 91–105.
- (17) Kim, S.-J.; Smith, M. D.; Darriet, J.; zur Loye, H.-C. *J. Solid State Chem.* **2004**, *177*, 1493–1500.
- (18) Doi, Y.; Hinatsu, Y. *J. Phys.: Condens. Matter* **2004**, *16*, 2849–2860.
- (19) Sakamoto, T.; Doi, Y.; Hinatsu, Y. *J. Solid State Chem.* **2006**, *179*, 2595–2601.
- (20) Doi, Y.; Hinatsu, Y. *J. Solid State Chem.* **2004**, *177*, 3239–3244.
- (21) Zhao, J. G.; Yang, L. X.; Mydeen, K.; Li, F. Y.; Yu, R. C.; Jin, C. Q. *Solid State Commun.* **2008**, *148*, 361–364.
- (22) Zhao, J. G.; Yang, L. X.; Yu, Y.; Li, F. Y.; Yu, R. C.; Fang, Z.; Chen, L. C.; Jin, C. Q. *J. Appl. Phys.* **2008**, *103*, 103706.

- (23) Young, R. A. *The Rietveld Method*; International Union of Crystallography/Oxford University Press: Oxford, U.K., 1995.

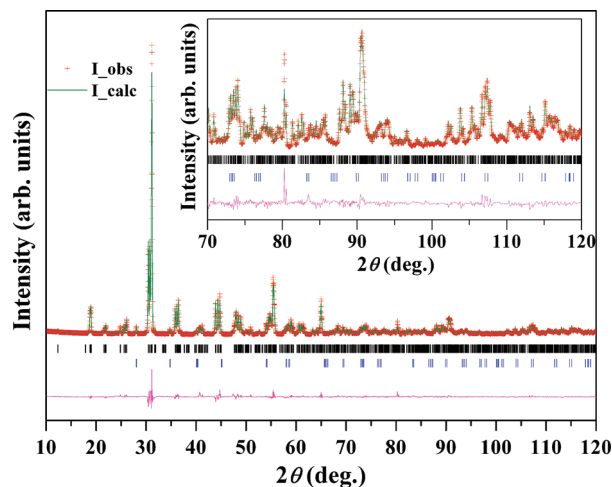


**Figure 2.** Experimental (open circle) and fitted (line) X-ray diffraction patterns for the 6M BaIrO<sub>3</sub>. The difference plot between observed and calculated patterns is shown at the bottom. The positions of the Bragg reflections are shown by the vertical lines. The inset shows the details of patterns in the range 70–120°.

arrange alternately and connect each other through the O anions in the corner. Figure 2 shows the observed and fitted XRD patterns of the 6M BaIrO<sub>3</sub>, and the inset shows the details in the range 70–120°. The data are analyzed with the Rietveld method. Except a few IrO<sub>2</sub>, the sample is basically a single phase. The lower vertical lines in Figure 2 are the Bragg reflections of IrO<sub>2</sub>. The existence of IrO<sub>2</sub> is due to the partial decomposition of the 9M BaIrO<sub>3</sub>, because the precursor is pure.<sup>21</sup> According to the refine results, the content of IrO<sub>2</sub> is about 2% in the whole compound. IrO<sub>2</sub> is a paramagnetic metal, with very small electrical resistivity and magnetic susceptibility in a large temperature range.<sup>24,25</sup> So the effect of IrO<sub>2</sub> on the physical properties of the 6M BaIrO<sub>3</sub> is very small. The obtained  $R_p$ ,  $R_{wp}$ , and  $R_{exp}$  factors are 6.86, 9.39, and 4.24%, respectively, which indicate the good consistency of the refined results. The lattice parameters are refined to be  $a = 5.7459(1)$  Å,  $b = 9.9289(2)$  Å,  $c = 14.3433(2)$  Å, and  $\beta = 91.340(1)^\circ$ . The shrinkage of volume of the 6M BaIrO<sub>3</sub> is about 3.6%, compared with the 9M form, which is approximately equal to that of the 6H BaRuO<sub>3</sub>.<sup>26</sup>

There is a large distortion in the BaO<sub>12</sub> icosahedrons, since the Ba–O distances are in the range of 2.671–3.392 Å and 2.576–3.247 Å for the Ba(1)O<sub>12</sub> and Ba(2)O<sub>12</sub> icosahedrons, respectively. The Ir(2)–Ir(2) distance is 2.719(1) Å for the two neighboring Ir cations in the Ir(2)<sub>2</sub>O<sub>9</sub> dioctahedron. The direct Ir(2)–Ir(2) distance of the 6M BaIrO<sub>3</sub> is larger than the values of 2.616(1) and 2.633(1) Å for the 9M form,<sup>10</sup> which is like that in BaRuO<sub>3</sub>.<sup>26</sup> There is a single IrO<sub>6</sub> octahedron in the 6M BaIrO<sub>3</sub>, which is different from the 9M phase. The longer direct Ir–Ir distance in the 6M BaIrO<sub>3</sub> is related with this single IrO<sub>6</sub> octahedron. The Ir(1) cation in the Ir(1)O<sub>6</sub> octahedron influences the Ir(2) cation through the O anion in the corner, which results in the longer direct Ir–Ir distance. For the two forms of BaIrO<sub>3</sub>, the Ir–Ir

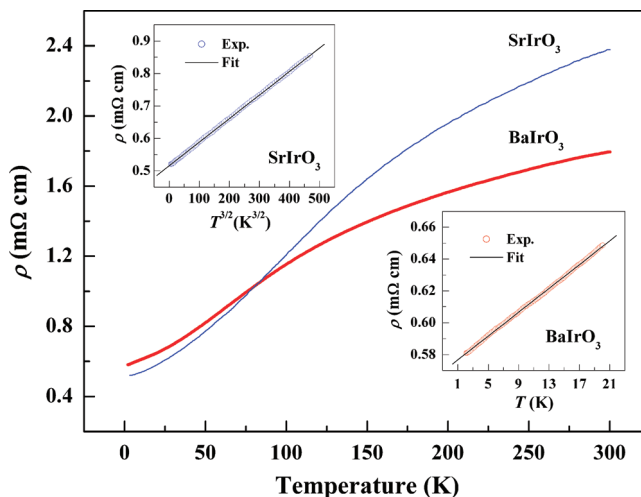


**Figure 3.** Temperature dependence of electrical resistivity of the 6M BaIrO<sub>3</sub> and the 6M SrIrO<sub>3</sub>. The inset in the bottom right corner shows the linear relationship of electrical resistivity versus temperature below 20 K. The other inset shows the linear relationship of electrical resistivity versus  $T^{3/2}$  below 60 K.

distances in the polyhedron are shorter than the separation in iridium metal (2.72 Å). Due to the large bulk modulus of 355 GPa for iridium metal,<sup>27</sup> there is strong repulsion between the adjacent Ir cations in BaIrO<sub>3</sub>. All the O–Ir–O angles deviate from 90 or 180°, which indicates that both the Ir(2)<sub>2</sub>O<sub>9</sub> dioctahedron and the Ir(1)O<sub>6</sub> octahedron are distorted from the idea ones. According to the interatomic distances and bond angles, it is deduced that the distortion degree of the 6M BaIrO<sub>3</sub> is larger than that of the 6H BaRuO<sub>3</sub> with the similar ion coordination.<sup>26</sup>

**Electrical Properties.** The temperature dependence of electrical resistivity of the 6M BaIrO<sub>3</sub> is shown in Figure 3. The 9M BaIrO<sub>3</sub> is a semiconductor for the polycrystal sample,<sup>28</sup> but the 6M BaIrO<sub>3</sub> maintains the metallic behavior down to the lowest temperature in our experiment. The inset in the bottom right corner of Figure 3 shows the linear relationship of electrical resistivity versus temperature below 20 K, which indicates that the  $\rho$ – $T$  curve follows the equation  $\rho = \rho_0 + AT$ , where  $\rho_0$  is 0.5730(1) mΩ cm and  $A$  is 3.731(6) μΩ cm/K. The residual resistivity ratio (RRR =  $\rho_{300K}/\rho_{T \rightarrow 0}$ ) for the 6M BaIrO<sub>3</sub> is approximately equal to 3, which is less than the value of 7 for the 6H BaRuO<sub>3</sub>.<sup>26</sup> So the metallicity of the 6M BaIrO<sub>3</sub> is worse than that of the latter, because of the larger distortion degree in crystal structure. There is a possible non-Fermi-liquid behavior in the 6M BaIrO<sub>3</sub>, due to the deviation from the equation  $\rho = \rho_0 + AT^2$  for the  $\rho$ – $T$  curve at low temperature. The influence of disorder from oxygen vacancy might exist in our 6M BaIrO<sub>3</sub> sample. However, post anneal in O<sub>2</sub> or N<sub>2</sub> atmosphere causes little effect on overall electrical properties. So the non-Fermi-liquid behavior in the 6M BaIrO<sub>3</sub> is an intrinsic property that is related to the crystal structure itself. We also obtained the relationship of electrical resistivity versus temperature of the 6M SrIrO<sub>3</sub>, with the results shown in Figure 3, as a comparison to that of the 6M BaIrO<sub>3</sub>. The

(24) Ryden, W. D.; Lawson, A. W.; Sartain, C. C. *Phys. Rev. B* **1970**, *1*, 1494–1500.

(25) Ryden, W. D.; Lawson, A. W. *J. Chem. Phys.* **1970**, *52*, 6058–6061.

(26) Zhao, J. G.; Yang, L. X.; Yu, Y.; Li, F. Y.; Yu, R. C.; Fang, Z.; Chen, L. C.; Jin, C. Q. *J. Solid State Chem.* **2007**, *280*, 2816–2823.

(27) Gschneidner, K., Jr. *Solid State Phys.* **1964**, *16*, 275–426.

(28) Kini, N. S.; Benti, A.; Ramakrishnan, S.; Geibel, C. *Physica B* **2005**, *359–361*, 1264–1266.

resistivity of the 6M SrIrO<sub>3</sub> could be described by the relationship of  $\rho$  versus  $T^{3/2}$ , as shown in the inset in the top left corner of Figure 3. This result is similar with that in the single crystal SrIrO<sub>3</sub>.<sup>29</sup> In fact, we synthesized the 6M Ba<sub>1-x</sub>Sr<sub>x</sub>IrO<sub>3</sub> by using high-pressure and high-temperature method and measured the temperature dependences of electrical resistivity (The results at  $0 < x < 1$  are not shown). When Sr content  $x$  is larger than 5/6, the relationship of  $\rho$  versus  $T$  follows the equation  $\rho = \rho_0 + AT^{3/2}$ .

Considering the similar structures between BaIrO<sub>3</sub> and BaRuO<sub>3</sub>, the metallic behavior of the 6M BaIrO<sub>3</sub> can be explained by some structural differences between 6M and 9M phases, referring that in BaRuO<sub>3</sub>. The 4H BaRuO<sub>3</sub> with the Ru<sub>2</sub>O<sub>6</sub> dioctahedron is metallic and there is a metal–insulator transition in the  $\rho$ – $T$  curve of the 9R phase with the Ru<sub>3</sub>O<sub>12</sub> trioctahedron,<sup>30,26</sup> which is consistent with the band structure around Fermi energy  $E_F$ .<sup>31</sup> The 6H BaRuO<sub>3</sub> have the structure and electrical properties similar to those of the 4H phase,<sup>26</sup> so it should have analogical electrical structure with the latter, although the band structure is not reported. According to the comparability between BaRuO<sub>3</sub> and BaIrO<sub>3</sub>, we connected the difference of electrical property between the 6M and 9M BaIrO<sub>3</sub> to their structural diversity. The d-electron orbitals of the 5d electrons have the larger spatial extension than those of the 3d one, so the oxide iridates should be metallic. However, the 9M BaIrO<sub>3</sub> is not a metal, for both the polycrystal and single-crystal samples,<sup>12,21</sup> although the short Ir–Ir distance in the Ir<sub>3</sub>O<sub>12</sub> trioctahedron is propitious to metallic behavior. The strong exchange interaction between the adjacent Ir cations results in the electron localization. The twisting and distortion of the Ir<sub>3</sub>O<sub>12</sub> trioctahedron give rise to the nonmetallic behavior, since they reduce the bandwidth.<sup>12</sup> The arrangement of Ir cations in the 6M BaIrO<sub>3</sub> is close to three-dimension due to a single-corner-shared IrO<sub>6</sub> octahedron between two Ir<sub>2</sub>O<sub>9</sub> dioctahedrons, unlike the quasi one-dimensional chain-type structure of the 9M form. The indirect interaction between Ir cations connected to each other through the vertex O anions, which can induce the unconventional electronic state and electrical property, is more important in the 6M BaIrO<sub>3</sub>. The electron localization in the Ir<sub>2</sub>O<sub>9</sub> dioctahedron, due to the Ir–Ir exchange interaction, is weaker than that in the Ir<sub>3</sub>O<sub>12</sub> trioctahedron of the 9M form, and the degree of twisting and distortion of the former is less than that of the latter. For the small distortion in crystal structure and high extend ability of orbital wave function, the 6M BaIrO<sub>3</sub> behaves the metallic property. As we know, among the ternary oxide iridates, only the ambient-pressure phase of SrIrO<sub>3</sub> (the 6M form), is a metal down to low temperature.<sup>9</sup> Our present work adds one new metallic iridate with the distorted hexagonal BaTiO<sub>3</sub> structure.

**Magnetic Properties.** Figure 4 shows the ZFC and FC temperature dependences of magnetic susceptibility of the

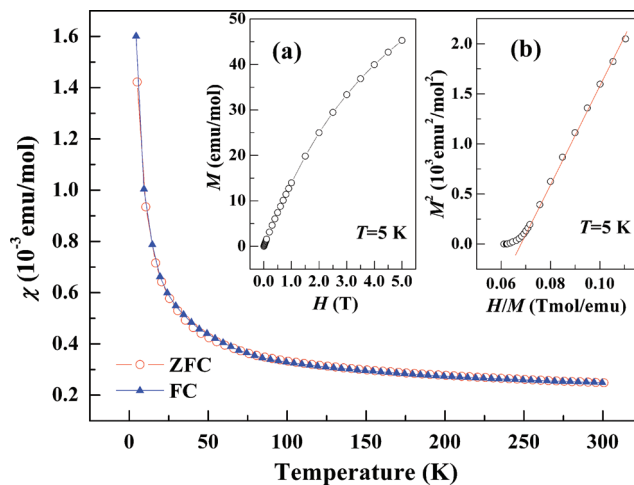


**Figure 4.** Temperature dependences of magnetic susceptibility of the 6M BaIrO<sub>3</sub>. The inset (a) shows the relationship of magnetization versus magnetic field at 5 K; (b) shows the relationship of  $M^2$  versus  $H/M$  converted from (a).

6M BaIrO<sub>3</sub>. There is no obvious deviation between ZFC and FC curves, indicating that the compound is basically not ferromagnetic. The magnetic susceptibility shows weak temperature dependence in the range 100–300 K and a slightly enhanced one at lower temperature. The 6M BaIrO<sub>3</sub> is electron correlation enhanced Pauli paramagnetic, and the value of magnetic susceptibility is equal to  $2.5 \times 10^{-4}$  emu/mol at 300 K. Taking into account the electron correlation, the data can be fitted to the following equation<sup>32</sup>

$$\chi = \frac{C}{T - \theta} + \chi_0(1 - AT^2) \quad (1)$$

where the parameter  $C$ ,  $\theta$ , and  $\chi_0$  are the Curie constant, paramagnetic Curie temperature, and the temperature independent susceptibility, respectively.  $A = (\pi^2 k_B^2/6) \{ [N'(E_F)/N(E_F)]^2 - [N''(E_F)/N(E_F)] \}$ , where  $N(E_F)$  is the density of states at Fermi level ( $E_F$ ) per atom,  $N'(E_F)$  and  $N''(E_F)$  are its first and second energy derivatives.<sup>32</sup> The effective magnetic moment  $\mu_{\text{eff}}$  per Ir atom is equal to  $0.276(1) \mu_B$ , as obtained from  $C$  through the formula  $\mu_{\text{eff}} = 2.83\sqrt{C}$ . The  $\mu_{\text{eff}}$  is smaller than the theoretical value of about  $1.73 \mu_B$  calculated in the spin-only model for the one unpaired 5d electron in the Ir<sup>4+</sup> cations, which indicates that the Ir<sup>4+</sup> cation loses partly local moment. This is attributed to the strong spin–orbit coupling and the improved itinerancy resulting from the direct interaction between two adjacent Ir cations. The small Ir moments are also found for the Ir<sup>4+</sup> cation in the 9M BaIrO<sub>3</sub> ( $0.13 \mu_B/\text{Ir}$ ),<sup>12</sup> perovskite SrIrO<sub>3</sub> ( $0.117 \mu_B/\text{Ir}$ ),<sup>23</sup> Sr<sub>2</sub>IrO<sub>4</sub> ( $0.50 \mu_B/\text{Ir}$ ),<sup>33</sup> and Sr<sub>3</sub>Ir<sub>2</sub>O<sub>7</sub> ( $0.69 \mu_B/\text{Ir}$ ).<sup>34</sup> The  $\theta$  of  $-3.1(1)$  K indicates that the interaction between the electronic spins on the nearest-neighbor sites is antiferromagnetic coupling in the Ir<sub>2</sub>O<sub>9</sub> dioctahedron. The fitting  $\chi_0$  and  $A$  are equal to  $2.47(2) \times 10^{-4}$  emu/mol and  $1.5(1) \times$

(29) Cao, G.; Durairaj, V.; Chikara, S.; DeLong, L. E.; Parkin, S.; Schlottmann, P. *Phys. Rev. B* **2007**, *76*, 100402.

(30) Rijssenbeek, J. T.; Jin, R.; Zadorozhny, Y.; Liu, Y.; Batlogg, B.; Cava, R. J. *Phys. Rev. B* **1999**, *59*, 4561–4564.

(31) Felser, C.; Cava, R. J. *Phys. Rev. B* **2000**, *61*, 10005–10009.

(32) Kaul, S. N.; Semwal, A.; Schaefer, H.-E. *Phys. Rev. B* **2000**, *62*, 13892–13895.

(33) Cao, G.; Bolivar, J.; McCall, S.; Crow, J. E.; Guertin, R. P. *Phys. Rev. B* **1998**, *57*, R11039–R11042.

(34) Cao, G.; Xin, Y.; Alexander, C. S.; Crow, J. E.; Schlottmann, P.; Crawford, M. K.; Harlow, R. L.; Marshall, W. *Phys. Rev. B* **2002**, *66*, 214412.

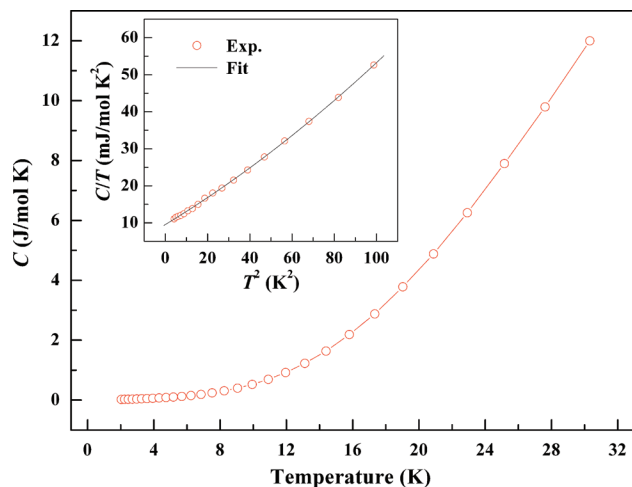


**Figure 5.** Low-temperature specific heat of the 6M BaIrO<sub>3</sub>. The inset shows the relationship of  $C/T$  versus  $T^2$ .

$10^{-6} \text{ K}^{-2}$ , respectively. The inset (a) of Figure 4 shows the relationship of magnetization versus magnetic field at 5 K, which confirms no long-range ferromagnetic order in the 6M BaIrO<sub>3</sub>. The inset (b) shows the Arrott plot, i.e. the  $M^2$ -( $H/M$ ) curve. The negative intercept on the  $M^2$ -axis, as obtained from the linear extrapolation of the high-field portion to  $H = 0$ ,<sup>35</sup> indicates that no spontaneous magnetization exists at 5 K.

**Specific Heat.** Figure 5 shows the low-temperature specific heat of the 6M BaIrO<sub>3</sub>. There is no any  $\lambda$ -type anomaly in the  $C$ - $T$  curve, indicating no long-range magnetic order or phase transition happening, being consistent with the magnetic measurements. The data below 10 K can be fitted to the equation

$$C/T = \gamma + \beta T^2 + \delta T^4 \quad (2)$$

where the first term is the electronic contribution, the second term is the phonon contribution according to the Debye approximation, and the third term is the deviation from the linear dispersion of the acoustic modes in extended temperature range. The  $C/T - T^2$  curve is shown in the inset of Figure 5. The Debye temperature  $\theta_D$  is equal to 304(2) K, as obtained from  $\beta$  through the formula  $\Theta_D = (1.944 \times 10^6 p / \beta)^{1/3}$ , where the atom number per chemical formula unit ( $p$ ) is equal to 5 for BaIrO<sub>3</sub>. The Sommerfeld constant  $\gamma$  of 9.5(1) mJ/molK<sup>2</sup> is obtained. So the Wilson ratio  $R_W$  is equal to 1.88(5), as calculated from  $\chi_0$  and  $\gamma$  through the formula  $R_W = 1/3(\pi k_B / \mu_B)^2 (\chi_0 / \gamma)$ , which is larger than the value of 1 for the free electron system,<sup>36</sup> indicating the enhancement of electron-electron correlation in the 6M BaIrO<sub>3</sub>.

## Summary

The 6M BaIrO<sub>3</sub> was synthesized using the high-pressure technique, and the XRD pattern, electrical resistivity, mag-

**Table 1.** Selected Bond Distances (Å) for 6M BaIrO<sub>3</sub>

bond	distance (Å)	bond	distance (Å)
Ba(1)-O(1) × 2	2.874(1)	Ir(1)-O(3) × 2	1.980(24)
Ba(1)-O(2) × 2	2.922(17)	Ir(1)-O(4) × 2	1.906(18)
Ba(1)-O(2) × 2	2.832(17)	Ir(1)-O(5) × 2	2.067(15)
Ba(1)-O(3) × 2	3.392(19)	Ir(1)-O(average)	1.984(19)
Ba(1)-O(4) × 2	2.671(15)		
Ba(1)-O(5) × 2	2.673(13)	Ir(2)-O(1)	2.205(27)
Ba(1)-O(average)	2.894(14)	Ir(2)-O(2)	2.033(14)
		Ir(2)-O(2)	1.966(15)
Ba(2)-O(1)	2.760(20)	Ir(2)-O(3)	2.072(21)
Ba(2)-O(2)	2.778(14)	Ir(2)-O(4)	2.160(20)
Ba(2)-O(2)	3.076(14)	Ir(2)-O(5)	1.966(16)
Ba(2)-O(3)	2.576(20)	Ir(2)-O(average)	2.067(19)
Ba(2)-O(3)	2.910(24)		
Ba(2)-O(3)	2.936(24)	Ir(2)-Ir(2)	2.719(1)
Ba(2)-O(4)	2.729(18)		
Ba(2)-O(4)	3.046(18)		
Ba(2)-O(4)	3.247(16)		
Ba(2)-O(5)	2.782(17)		
Ba(2)-O(5)	2.957(17)		
Ba(2)-O(5)	3.232(13)		
Ba(2)-O(average)	2.919(18)		

**Table 2.** Selected Bond Angles (deg) for 6M BaIrO<sub>3</sub>

bond	angle (deg)	bond	angle (deg)
O(1)-Ir(2)-O(2)	80.6(8)	O(3)-Ir(1)-O(3)	180.0(2)
O(1)-Ir(2)-O(2)	82.1(8)	O(3)-Ir(1)-O(4)	89.4(7)
O(1)-Ir(2)-O(3)	97.4(5)	O(3)-Ir(1)-O(4)	90.6(7)
O(1)-Ir(2)-O(4)	167.3(4)	O(3)-Ir(1)-O(5)	86.8(7)
O(1)-Ir(2)-O(5)	88.7(4)	O(3)-Ir(1)-O(5)	93.2(7)
O(2)-Ir(2)-O(2)	81.0(9)	O(4)-Ir(1)-O(4)	180.0(6)
O(2)-Ir(2)-O(3)	97.4(9)	O(4)-Ir(1)-O(5)	84.4(6)
O(2)-Ir(2)-O(3)	177.5(9)	O(4)-Ir(1)-O(5)	95.6(6)
O(2)-Ir(2)-O(4)	90.9(7)	O(5)-Ir(1)-O(5)	180.0(3)
O(2)-Ir(2)-O(4)	87.8(7)		
O(2)-Ir(2)-O(5)	88.5(7)	Ir(1)-O(3)-Ir(2)	158.9(9)
O(2)-Ir(2)-O(5)	167.1(8)	Ir(1)-O(4)-Ir(2)	159.8(8)
O(3)-Ir(2)-O(4)	94.1(7)	Ir(1)-O(5)-Ir(2)	163.7(6)
O(3)-Ir(2)-O(5)	92.8(7)	Ir(2)-O(1)-Ir(2)	76.2(6)
O(4)-Ir(2)-O(5)	96.3(7)	Ir(2)-O(2)-Ir(2)	85.7(6)

netic susceptibility, and specific heat were obtained. Structural data indicated that the 6M BaIrO<sub>3</sub> crystallizes into the distorted hexagonal BaTiO<sub>3</sub> structure. The measurements of electrical and magnetic properties showed that the 6M BaIrO<sub>3</sub> is an abnormal paramagnetic metal that is deviated from the Fermi liquid behavior. The large Wilson ratio indicated an electron-electron correlation in the compound.

**Acknowledgment.** We thank Prof. C. Dong and H. Chen of Institute of Physics, Chinese Academy of Sciences for their help in XRD measurement and analysis. We are grateful for the support from NSF and Ministry of Science and Technology of China through the research projects.

**Supporting Information Available:** Atomic coordinates and selected bond distances and angles of the 6M BaIrO<sub>3</sub> (CIF). This material is available free of charge via the Internet at <http://pubs.acs.org>.

IC801707M

(35) Arrott, A. *Phys. Rev.* **1957**, *108*, 1394–1396.

(36) Wilson, K. G. *Rev. Mod. Phys.* **1975**, *47*, 773–840.